INVESTIGATION ON ACCELERATED IMPEDANCE SPECTRUM MEASUREMENT METHOD WITH MULTISINE SIGNAL STIMULATION

Marek Niedostatkiewicz, Romuald Zielonko

Gdansk University of Technology, Faculty of Electronics, Telecommunication and Informatics, G. Narutowicza 11/12, 80-233Gdańsk, Poland (niedost@eti.pg.gda.pl, ✉ zielonko@eti.pg.gda.pl, +48 58 347 2255)

Abstract

The paper presents an investigation on the accelerated impedance spectrum measurement method, oriented at parameter identification of technical objects modelled by a linear equivalent circuit, *e.g.* anticorrosion coatings. The method is based on multisine signal stimulation of an object and response analysis by triangle window filter-banks. It has several advantages, as compared with conventional point-by-point spectrum measurement. The method was implemented in an experimental measurement system based on a DAQ card. The achieved experimental results are discussed and compared with simulation results, in terms of measurement time reduction and accuracy.

Keywords: impedance spectroscopy, multisine measurement signals, anticorrosion coatings diagnosis.

1. Introduction

The modelling of many technical and biological objects with electrical circuits has recently become very popular. The reason is that such modelling allows monitoring and diagnosing of their state with the aid of well-developed tools and methods designed for electrical circuits. Particularly popular is the impedance parameters identification of objects modelled by multi-element, two-terminal equivalent circuits: anticorrosion coatings [1, 10], materials [2], sensors [3], reinforced concrete constructions [4] and biological objects like physiological fluids and tissues [5].

Impedance spectroscopy is the conventional method of finding equivalent circuit parameter values. It is based on measurement of the object impedance spectrum, usually point-by-point with single frequency impedance analyzers and fitting the parameter-dependent model to measurement data, usually by the Complex Non-linear Least Squares (CNLS) method [6].

The main disadvantage of such process is the spectrum measurement time. The frequency range starts, in the case of some objects, from the order of mHz and even μHz, thus implicating a very long measurement time (order of hours).

The need for reduction of impedance spectrum measurement time, even at the cost of accuracy, is motivated by several technical and economical reasons. Firstly, field measurements lasting hours are both unpractical and very expensive. Secondly, there is a need for impedance spectrum measurement of dynamic or quasi-dynamic objects, where conventional, time consuming methods are not reliable due to object's parameter variation during measurement.

The impedance spectrum of linear objects can be measured, according to the superposition principle, in one cycle (potentially faster) with a multisine stimulus.

However, the conventional multisine approach to DFT method [7, 8] is inconvenient to implement in practice due to problems with the long period of multisine. The measurement of

coherently sampled multisine measurement with proper DFT window length could last longer than the point-by-point, single frequency method.

To circumvent these disadvantages, the authors have proposed the digital filter bank analysis of multisine signals with triangle window low-pass FIR filters. The idea of the method, several test multisine signals, the simulation results and comparison with the single frequency DFT method (used in modern impedance analyzers) were discussed in [9]. The method was proven, by means of simulation, to be faster than other methods currently used.

This paper describes the theoretical basics and practical verification of the method in a dedicated virtual impedance analyser, based on a data acquisition (DAQ) card. The structure of the system is presented and the experimental results are compared with the simulations conducted before.

2. Theoretical basics of the method

2.1. Measurement idea

The measurement idea of the multisine method with filter bank analysis is presented in Fig. 1. The K-component multisine stimulation signal $u[n]$ is synthezised in the summation node in a sample-by-sample (iterative) manner. Thus, there is no necessity of storing a long multisine period in the memory, as in conventional Arbitrary Waveform Generators. The multisine is characterised by pulsations ω_k and complex amplitudes $A_{\omega k}$.
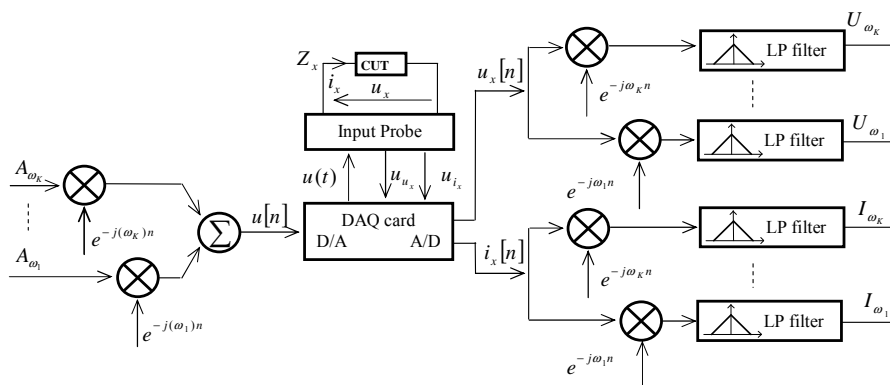

Fig. 1. Illustration of the measurement idea.

The Input Probe applies the stimulus voltage to the circuit under test (CUT) and extracts the signals proportional to impedance voltage u_{ux} and current u_{ix}. Both signals are sampled simultaneously producing the digital forms $u_x[n]$ and $i_x[n]$, which are analyzed by two identical digital filter banks. Every filter bank channel is built from a modulator and a low-pass filter. The modulator shifts the spectrum in the frequency domain, according to the modulation principle. If we denote K-component multisine signal (*e.g.* $u_x[n]$ and $i_x[n]$) as:

$$x[n] = X_0 + \sum_{k=1}^{K}(X_k e^{j\omega_k n} + X_k^* e^{-j\omega_k n}),$$
(1)

then the signal after modulation by ω_s in s-th frequency filter bank channel is:

$$x_{\omega_s}[n] = x[n] \cdot e^{j\omega_s n} = X_0 \cdot e^{-j\omega_s n} + \sum_{k=1}^{K}\left(X_k e^{j(\omega_k-\omega_s)n} + X_k^* e^{-j(\omega_k+\omega_s)n}\right) =$$

$$= X_0 \cdot e^{-j\omega_s n} + \sum_{k=1}^{s-1}(X_k e^{j(\omega_k-\omega_s)n} + X_k^* e^{-j(\omega_k+\omega_s)n}) + X_{k=s} + \sum_{k=s+1}^{K}\left(X_k e^{j(\omega_k-\omega_s)n} + X_k^* e^{-j(\omega_k+\omega_s)n}\right). \tag{2}$$

Equation (2) shows that if modulator pulsation ω_s is equal to the multisine component pulsation ω_k, the DC value at output of modulator will be the amplitude $X_{k=s}$ of component with frequency $f_{k=s}$. Thus, the spectral component corresponding to modulating frequency is shifted to DC. Then its complex amplitude is extracted by low pass filter present in every filter bank channel [10]. Filter-banks calculate the complex amplitudes $U_{\omega k}$ and $I_{\omega k}$ of the frequency components, corresponding to the frequencies present in the stimulus. The complex division of these values allows calculating the impedance spectrum of an object for a given set of frequencies.

2.2. Multisine stimuli

A verification of the method has been conducted for the 4 multisine signals, denoted S1-S4. Signals S1-S3 consist of 14 sines covering the 2-decade frequency range.

The signal S1 has a lin-log distribution of frequencies (linear inside a decade and logarithmic in decades). None of the sine periods is a multiplication of another sine period. As a consequence, the multisine period is extremaly long, of the order of $7,5 \cdot 10^{17}$ samples. The signal was chosen to check the method in very unfavourable conditions.

Table 1. Frequency and normalised period of signal S1 components.

f [kHz]	0.101	0.203	0.304	0.409	0.510	0.707	0.815	1.008	2	4.129	6.095	8533	9.846	11.64
$\hat{T}_k$	1268	631	421	313	251	181	157	127	64	31	21	15	13	11

The signal S2 is the heuristically optimized version of signal S1 with small frequency shifts. As a result, the multisine period is shorter ($2,3 \cdot 10^7$ samples) and the period of the lowest frequency component is a multiplication of several periods of other frequencies. The signal was chosen to test the effectiveness of multisine frequencies optimization.

Table 2. Frequency and normalised period of signal S2 components.

f [kHz]	0.1	0.2	0.3	0.4	0.5	0.699	0.8	1	2	4	6.095	8	9.846	11.63
$\hat{T}_k$	1280	640	427	320	256	183	160	128	64	32	21	16	13	11

The signal S3 is an optimal multisine with a very long period equal to the doubled period of the first sine. This signal can be filtered even with a simple rectangular window filter with the length equal to that period (2580 samples), covering all the periods of components. The frequencies in signal S3 were formed by summing two geometric progressions, so the frequency distribution is quasi-logarithmical. The signal was chosen to test the precision of the method in optimal, yet very difficult to obtain conditions.

Table 3. Frequency and normalised period of signal S3 components.

f [kHz]	0.1	0.2	0.25	0.4	0.5	0.8	1	1.6	2	3.2	4	6.4	8	12.8
$\hat{T}_k$	1280	640	512	320	256	160	128	80	64	40	32	20	16	10

The signal S4 is a simple logarithmical distribution of 25 frequencies (8 per decade) covering the 3-decade frequency range. The frequencies form a geometric progression:

$$a_{k+1} / a_k = a_k / a_{k+1} = q_f, \qquad a_k = a_1 q_f^{k-1}, \tag{3}$$

with first element and ratio:

$$a_1 = f_{\min}, \qquad q_f = \sqrt[K-1]{f_{\max} / f_{\min}}, \qquad q_f > 1. \tag{4}$$

If we denote the number of logarithmic signal components as *K*, number of frequency decades as *D* and the number of points per decade as *L*, it can be shown that:

$$K = L \cdot D + 1, \qquad q_f = \sqrt[L \cdot D]{10^D} = \sqrt[L]{10}. \tag{5}$$

The signal S4 was chosen to test the method in case of simple technical frequency scale in 3-decade range.

All the signals above have been until now tested by means of simulation and described in previous papers by authors (*e.g* [9]). The research has shown that for such signals the multisine component phase shift optimisation is not very important.

$$\Phi_k = \frac{\pi (k-1) k}{K}. \tag{6}$$

However, the Schroeder equation (6) [11] concerning the angle of the multisine component has been used.

2.3. Triangle window filter bank analysis

A digital, low pass filter calculates the average value at the output of modulator (Fig. 2), being the complex amplitude of the multisine component with frequency equal to modulating frequency. Although the task seem to be frequency domain related, the time-domain optimized filters with sharp step response and fast impulse response need to be used, as the average must be calculated as soon as possible in predictable time in order to accelerate measurements.
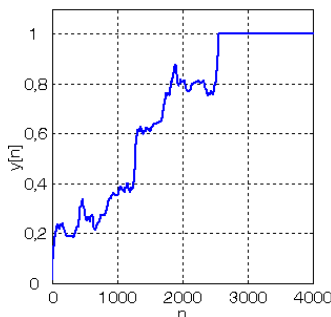

Fig. 2. The settling of normalized value at the output of an exemplary FIR filter with a window length of 2580 samples.

Finite impulse response (FIR) filters were chosen, due to their performance, stability, and settling time equal to the filter window length.

In preliminary investigations, rectangle window Moving Averager (MA) filters have been chosen, described by the equation:

$$y[n] = \frac{1}{M} \sum_{k=0}^{M-1} x[n-k]. \tag{7}$$

Their frequency characteristic is:

$$H(j\omega) = \sin\left(\frac{\omega M}{2}\right) / \left(\frac{\omega M}{2}\right).$$ (8)

MA filters can be implemented recursively, thus circumventing the main FIR disadvantage – amount of calculations required due to long filter kernel:

$$y[n] = \frac{1}{M} x[n] - \frac{1}{M} x[n-M-1] + y[n-1].$$ (9)

However, their spectral selectivity has been insufficient, so the triangle window filters have finally been introduced. The triangle window filter frequency response is given by the equation:

$$H(j\omega) = \sin^2\left(\frac{\omega M}{2}\right) / \left(\frac{\omega M}{2}\right)^2.$$ (10)

The normalized frequency response of both filters is presented in Fig. 3. Although a triangle window filter has a wider main lobe than the MA, it has better attenuation of higher frequencies, desirable in case of a multisine signal with a wide frequency range.
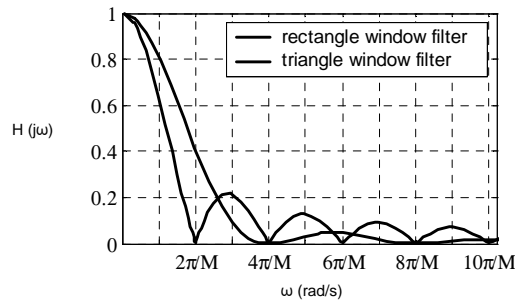

Fig. 3. Rectangle and triangle window filter characteristics.

The triangle window, being the pulse response of the *M*-length filter (10) is a convolution of two rectangular widows of *M/2*-length:

$$h_{triangle}(t) = h_{rectangle}(t) * h_{rectangle}(t).$$ (11)

It means that the *M*-length triangle filter can be implemented very efficiently; instead of time-domain convolution of signal with triangle window kernel, the same result is obtained by cascade connection of two *M/2*-length rectangular filters. In practice, the modulator outputs are filtered twice with a recursively implemented (8) *M/2*-length MA filter.

Filter characteristics are heavily dependent on filter length. The longer the filter kernel is, the better selectivity is achieved, yet, the measurement time is longer. Moreover, the earlier experiments have shown that the problem with filter selectivity usually occurs for the lowest frequency of the multisine, so it is desirable that the filter length be a multiplication of T_1.

On the other hand, the filters with *M*-long kernel stabilise after *M* samples, so the impedance measurement time is at least *M* samples long. In order to achieve measurement acceleration, the filter length *M* must be kept lower than the single-frequency measurement time which is similar to the sum of periods in the signal:

$$t_{meas.} \geq \sum_{i=1}^{N} T_i = \sum_{i=1}^{N} \frac{1}{f_i}.$$ (12)

By fulfilling the conditions described above, the potential measurement acceleration ratio for the signals S1-S3 are presented in Table 4.

Table 4. Frequency and normalised period of signal S3 components.

Signal	S1	S2	S3
Number of components	14	14	14
Filter-bank measurement time [samples]	2536	2560	2560
Aprox. DFT measurement time [samples]	3504	3551	3558
Measurement acceleration ratio	27%	28%	28%

3. The measurement system

The experimental measurement system was designed according to the idea presented in Fig. 1. It has the form of a virtual instrument based on PCI-6111E data acquisition card and a dedicated input impedance probe. The architecture of the system is presented in Fig. 4. There are 2 hardware blocks (input impedance probe, data acquisition card) and a dedicated software block.
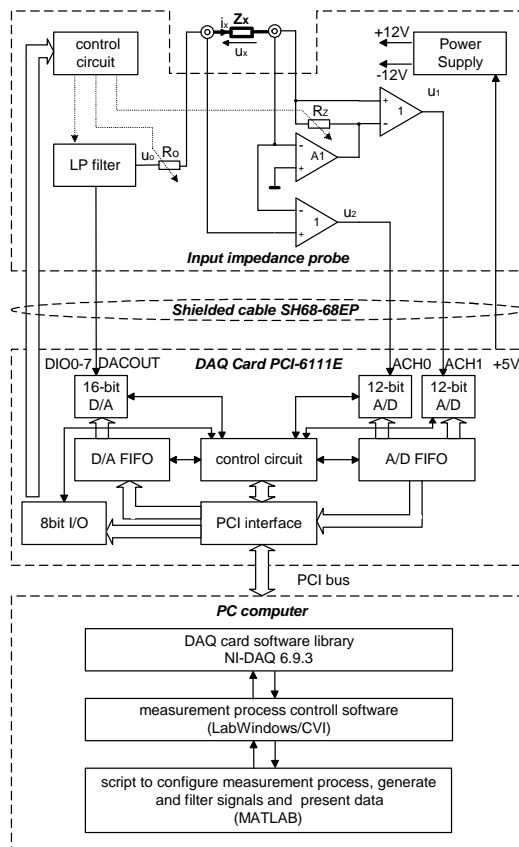

Fig. 4. Architecture of the measurement system.

The input impedance probe does the analogue-analogue conversions as described in measurement idea chapter: conditioning of the stimulus and extracting the signals proportio-

nal to current and voltage at the object. The probe is configured by 8 digital lines – the configured items are: the resistors in the current-voltage converter, analogue filters cut-off frequency, *etc*. The object (Circuit Under Test) can be placed in terminal clamps on the casing of the probe or connected via a dedicated socket.

Fig. 5. View of the setup with an experimental impedance analyzer.

The Data Acquisition Card (DAQ) placed inside the PC-class computer samples coherently the two extracted signals proportional to current and voltage and synthesizes the stimulus via the DDS (Direct Digital Synthesis) method. Moreover, the card generates the control signals to configure the measurement probe. The probe and the DAQ board are connected with a shielded SH68-68EP cable. Such a design allows to handle sensitive signals in high impedance circuits in the Input Probe shielded box, far from the noisy PC inside.

A laboratory setup with the experimental measurement system and a Digital Storage Oscilloscope (DSO) is presented in Fig. 5. There is an exemplary multisine stimulus present in the DSO display. The impedance object built from discrete RC-elements is placed in the terminal clamps of the impedance probe. The PC screen shows the panels of system software. The exemplary oscillogram of the logarithmic 14-component 2-decades multiharmonic stimulus and the response are presented in Fig. 6.
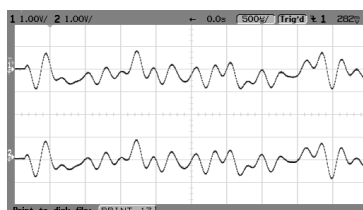

Fig. 6. Examplary oscillograms voltage (upper) and current (lower) signals for logarithmic multisine with 14 frequencies in 2-decades.

The software of the experimental system is a 3-layer solution, designed in 2 programming environments: Matlab and LabWindows/CVI.

The main functional software of the virtual impedance spectrum meter was written in the Matlab environment as a script (m-file). The script realises the measurement process according to the configuration data written in a text batch file, prepared by the user. The configuration involves: multisine components amplitude and frequency, sampling frequency, impedance probe configuration, type of filtering, filter window length, and the form of result presentation.

For the given set of frequencies the script calculates the measurement time, actual frequencies of multisine components (the frequency grid is dependent on the sampling frequency), component phase shift (according to Schroeder's equation) and finally, a record of stimulus samples.

Then, the measurement process control software DAQ measure is invoked. The software, written in LabWindows/CVI, controls the measurement itself – it configures the generation of the stimulus on the basis of data prepared by the script. It configures the acquisition of voltage and current responses by the ADC, reads the waveform and writes data on disk. The DAQ card operations are supervised by the NI-DAQ library, which handles the DAQ card in the operating system of a PC and offers a general programming interface for DAQ card operations.

After the sampling is finished, the Matlab script continues the operation, modulating and filtering the signals, thus calculating the complex impedance spectra which can be presented in various forms: Bode plot of magnitude and phase, Nyquist plot or tabular form.

The software architecture has several advantages in terms of a scientific experiment. The use of Matlab allows to batch process and automatize several experiments in the same circuit with different stimuli or analysis methods. Moreover, the results (and indirect results) stay present in the Matlab environment after finishing the measurement, thus allowing *e.g.* to filter the same set of data in different conditions without the need to repeat the experiment itself.

4. Experimental verification of the method

The aim of the experimental verification was to validate the conclusions from simultations decribed in [8]. Thus, the same test object and signals S1-S3 were used, to compare the spectrum measurement in 2-decade frequency range with different filtering and multisine designing strategies. The second part of the experimental verification is the 3-decade spectrum measurement with a conventional, logarithmical distribution of 25 frequencies.

4.1. Test object

The spectrum measurement method has been tested on the Randles model in the form a of simple 3-element two-terminal shown in Fig. 7 with the impedance described by the formula:

$$Z(s) = \frac{\left(R_s R_p C_p\right)s + \left(R_s + R_p\right)}{\left(R_s R_p\right)s + 1} \; . \tag{13}$$
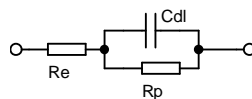

Fig. 7. The Randles model.

The Randles model is very popular in electrochemistry (*e.g.* to model early stages of paint substrate corrosion) and it is frequently used as a test engine to compare various impedance spectrum estimation methods. The model equivalent circuit was built from discrete RC elements: $R_e = 99{,}95\Omega$, $R_p = 99{,}97\Omega$, $C_{dl} = 4{,}68\mu F$.

4.2. Spectrum measurement in 2-decade frequency range with MA and triangle window filters

The spectrum measurement was conducted for 3 signals S1-S3 and 2 types of filters: a MA filter with rectangular window and a triangle window filter. The results are presented in the form of Bode and Nyquist plots. The thin line represents the theoretical spectrum for given

element values, whereas the thick line connects the impedance values at measurement frequencies (circles).

The plots for worst case – non-optimized multisine and MA filter are in Fig. 8. The measurement error is rather high (up to a few percent) which can be seen especially on the Nyquist plot.
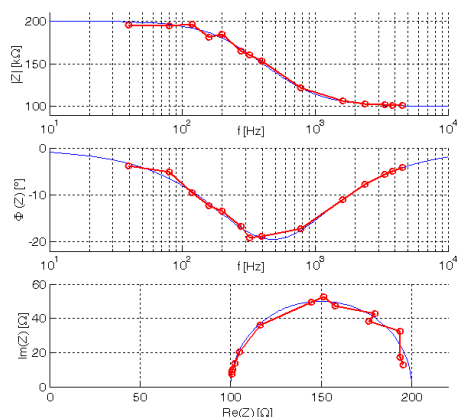

Fig. 8. Bode and Nyquist plot of the impedance spectrum, signal S1, MA filter.

The Fig. 9 presents the best result – measurement with optimal signal S3 with a specific distribution of frequencies (which can be seen as placement of measurement points on Bode plots) and a MA filter of length equal to that multisine period. It can be seen that in such a case the measurement points match the theoretical spectrum – the maximum magnitude relative error (difference between theoretical and experimental value) is less then 0.18%.
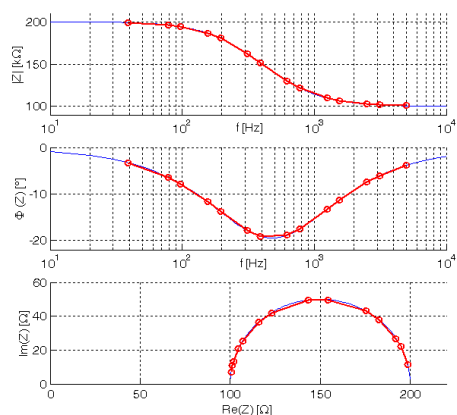

Fig. 9. Bode and Nyquist plot of impedance spectrum, signal S3, MA filter.

The measurements with signal S2 have confirmed that a heuristic optimisation of frequency distribution in the multisine, decreases the measurement error to approx. 0.25%. The experiments with triangle window filters have shown that the same accuracy can be obtained for a non-optimised signal S1 without the need of heuristic optimization.

The experiments have confirmed the simulation results, that for specific, optimal signals the MA filter is a good choice, but for an arbitrary (non-optimized) set of frequencies the triangle window filter is better.

4.3. Measurement with triangle window filters and 25 components 3-decade frequency range multisine.

In the second part of the experiment, the multisine had a logarithimic distribution of frequencies, covering the 3-decade range (10Hz-10kHz) with 25 sines (8 per decade). Such distribution of spectrum measurement points is common in practice. According to previous results, the triangle window filter has been applied.

The experiments were conducted with several values of filter length. The lowest filter length was set as not less than a doubled period of the lowest frequency. In case of recursive triangle window filter of length $M=2T_1$, a rectangular MA sub-filter of length $M/2$ "catches" at least 1 period of T_1.

Unfortunately, the measurement error for first decade was too high for precise measurement. The 3D plot (Fig. 9) shows how the magnitude and phase of impedance change (fluctuate) at the output of filter bank channels in case of continous stimulus signal. It is obvious, that the selectivity of filters is insufficient and low frequency components (f_2, f_3,…) interfere with each other.
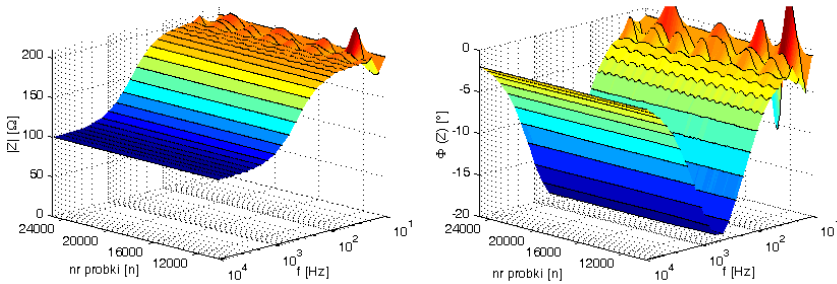

Fig. 10. Changes of impedance spectra (magnitude and phase); signal S4, triangle window filter $M=2T_1$.

The measurement accuracy has been increased by using longer filter windows in channels 2-25. The plot of filter bank output (Fig. 10) for $M=3,2T_1$ shows that fluctuations in magnitude are very low – only the phase spectrum has some minor instabilities.
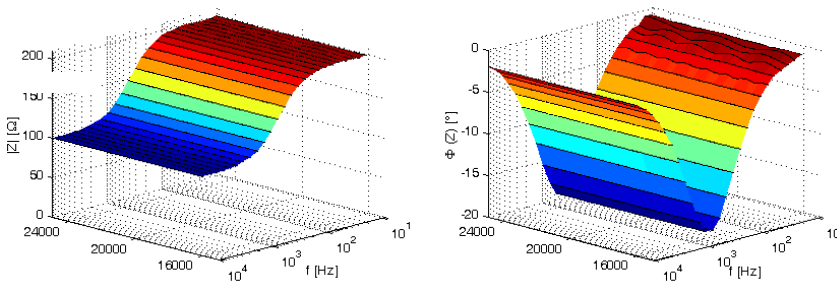

Fig. 11. Changes of impedance spectra (magnitude and phase); signal S4, triangle window filter $M=3,2T_1$.

Consequently, the Bode and Nyquist plots of theoretical and experimentally-measured impedance spectra are almost undistinguishable (Fig. 11).
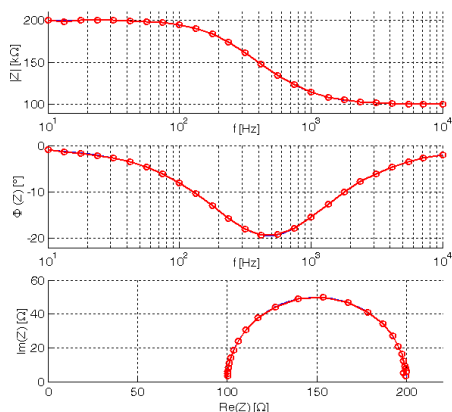
Fig. 12. Bode and Nyquist plot of impedance spectrum, signal S4, triangle window filter M=3,2T_1.

The measurement time for 3 examined lengths of the filter is presented in Table 5 and compared with the single-frequency DFT method. Moreover, the measurement acceleration ratio is calculated.

Table 5. Comparison of spectrum measurement time between filter bank method and single-frequency DFT method.

Filter length	Measurement time		
	Filterbank	DFT method	Difference
$M = 2\hat{T}_1$	200 ms	400 ms	-50%
$M = 3\hat{T}_1$	300 ms	400 ms	-25%
$M = 3,2\hat{T}_1$	320 ms	400 ms	-20%

In order to present the measurement error, the relative magnitude error and absolute phase error have been calculated for each of 25 multisine components. The plots of error values for 3 tested filter lengths are shown in Fig. 13.
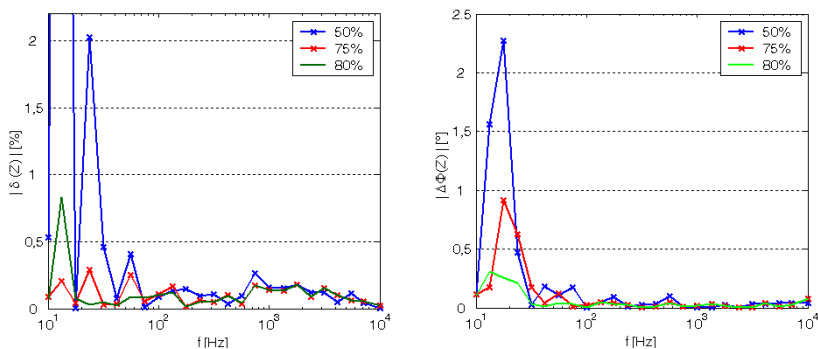

Fig. 13. Relative magnitude error and absolute phase error of impedance spectra measured with signal S4 for 3 different measurement acceleration ratios.

5. Conclusions

The experimental verification in a dedicated measurement system has confirmed the possibility of accelerating impedance spectrum measurement in few decades of frequency with logarithmic distribution of spectrum sampling points. The method, based on multisine stimulation and filter-bank analysis circumvents the disadvantages of conventional single-frequency or multisine and DFT approaches. The experimental results are in correlation with simulation results from earlier research [9]. The accuracy of the method is comparable with commercial single-frequency impedance meters.

The experiments with various values of filter length have confirmed the main advantage of the filter-bank method: the interchangeability of accuracy and spectrum measurement time. Thus, depending on the required accuracy, the acceleration ratio can be in the range of 20-50%. The cost of high acceleration ratio is decreased accuracy in the 1st decade (the 2nd and 4th component of multisine in Fig. 12). However, the relative magnitude error for such quick, rough measurement is still on the acceptable level of few percent.

Although the absolute times in Table 5 are of the order of ms, it should be stated that the achieved results would be kept the same in the discrete domain if the sampling frequency was much lower. Then, in case of very low-frequency 3-decade spectrum measurement the filter bank method could save hours of measurement time.

Although the method and system were oriented at anticorrosion coating diagnosis, the general results can be useful for the acceleration of parameter identification of several different objects and phenomena modelled by electric circuits.

References

[1] P.L. Bonora, F. Deflorian, L. Federizzi: "Electrochemical Impedance Spectroscopy as a tool for investigating underpaint corrosion". *III International Symposium on Electrochemical Impedance Spectroscopy*, Nieuwpoort, Belgium, 1995.

[2] B.W. Licznerski, K. Nitsch: "Impedance Spectroscopy in the investigation of electronic materials". *USA/Poland Microelectronics Symposium*, Wroclaw, Poland, 1995.

[3] L.J. Golonka, B.W. Licznerski, K. Nitsch, H. Teterycz: "Thick-film humidity sensors". *18th International Spring Seminar on Electronic Technology*, ISSE, Czech Republic, 1995.

[4] S. Hong, R.S. Harichandran: "Sensors to monitor CFRP/Concrete Bond in Beams Using electrochemical Spectroscopy". *J. Compos. For Constr.*, vol. 9, 2005.

[5] R. Bragos, R. Blanco-Enrich, O. Casas, J. Rosell: "Characterisation of dynamic Biologic Systems Using Multisine Based Impedance Spectroscopy". *IEEE IMTC* Conference, Budapest, Hungary, 2001.

[6] B.A. Boukamp: "Non-linear Least Square Fit for analysis of immitance data of electrochemical systems". *Solid State Ionics,* vol. 20, 1986.

[7] J. Hoja, G.Lentka: "Analyzer for spectroscopy of low-impedance objects". *Metrol. Meas. Syst.,* vol. XVI, no. 1, 2009, pp. 19- 31.

[8] D. Smith: "The acquisition of Electrochemical Response Spectra by On-Line Fast Fourier Transform". *Analytical Chemistry*, vol. 48, 1976.

[9] R. Zielonko, M. Niedostatkiewicz: "Accelerated multisine impedance method directed at diagnosis of anticorrosion coatings". *XVIII IMEKO World Congress*, Brazil, 2006.

[10]J. McClellan, R. Schafer, M. Yoder: *DSP First a Multimedia Approach*, Prentice-Hall, 1996.

[11]R. Guyla, J. Shoukens, Laszlo: "An Efficient Nonlinear Least Square Fitting Algorithm". *IEEE Trans. on Instrumentation and Measurement*, vol. 51, no. 4, 2002, pp. 1196-1201.